Observed Recent Trends in Tropical Cyclone Rainfall Over Major Ocean Basins

K. M. Lau

Laboratory for Atmospheres, NASA Goddard Space Flight Center

And

Y. P. Zhou
Goddard Earth Sciences Technology and Research
Morgan State University
NASA Goddard Space Flight Center

Submitted to Journal of Geophysical Research – Atmosphere
July 2011

Corresponding author: K. M. Lau, Laboratory for Atmospheres, NASA, Goddard Space Flight Center, Greenbelt MD, 20771. Email: William.k.lau@nasa.gov

Abstract

In this study, we use Tropical Rainfall Measuring Mission (TRMM) and Global Precipitation Climatology Project (GPCP) rainfall data together with historical storm track records to examine the trend of tropical cyclone (TC) rainfall in major ocean basins during recent decades (1980-2007). We find that accumulated total rainfall along storm tracks for all tropical cyclones shows a weak positive trend over the whole tropics. However, total rainfall associated with weak storms, and intense storms (Category 4-5) both show significant positive trends, while total rainfall associated with intermediate storms (Category1-3) show a significant negative trend. Storm intensity defined as total rain produced per unit storm also shows increasing trend for all storm types. Basin-wide, from the first half (1980-1993) to the second half (1994-2007) of the data period, the North Atlantic shows the pronounced increase in TC number and TC rainfall while the Northeast Pacific shows a significant decrease in all storm types. Except for the Northeast Pacific, all other major basins (North Atlantic, Northwest Pacific, Southern Oceans, and Northern Indian Ocean) show a significant increase in total number and rainfall amount in Category 4-5 storms. Overall, trends in TC rainfall in different ocean basins are consistent with long-term changes in the ambient large-scale environment, including SST, vertical wind shear, sea level pressure, mid-tropospheric humidity, and Maximum Potential Intensity (MPI). Notably the pronounced positive (negative) trend of TC rainfall in the North Atlantic (Northeast Pacific) appears to be related to the most (least) rapid increase in SST and MPI, and the largest decrease (increase) in vertical wind shear in the region, relative to other ocean basins.

Introduction

Tropical cyclones (TC) are among nature's most destructive forces. Whether the number and the intensity of TCs have changed or will change in a warming climate has been the subject of many studies. However the issue is far from settled, due to large interannual and interdecadal variability in the frequency and intensity of TCs and limitation in the availability and quality of global long-term historical records of TCs [Pielke et al., 2005; Shepherd and Knutson, 2006; Landsea et al., 2006; 2008; Knutson et al., 2010]. Despite large uncertainties in observed long-term TC frequency and intensity change, numerical models have predicted that TC related rainfall rates are likely to increase with greenhouse warming [Knutson and Tuleya, 2004; Bengtsson, 2007]. Such models have also projected substantial increase in storm-centered rainfall in the late 21st century in the range of +3-37%, resulting from increased evaporation from the warmer ocean and increased moisture in the atmosphere. For TC's, where moisture convergence plays a key role, increased available moisture in the atmosphere is expected to lead to greater rain rates.

Previous studies found that the frequency of extreme rainfall has increased in the last several decades over land from land-based precipitation data set [Karl and Knight, 1998; Groisman et al., 2004], as well as over the tropical oceans based on long-term satellite precipitation data [Lau and Wu, 2007]. In the coastal regions of South China and southeastern United States, TCs account for a significant portion of total rainfall, and even more so for extreme rainfall, and an increase in major TCs may be related to extreme rain events [Wu and Zhai, 2007; Shepherd et al, 2007]. Lau at el. [2008] recently studied the relationship between TC related rainfall and extreme rain events in North Atlantic and Northwest Pacific using nearly 30-year of GPCP pentad data. They found that TCs contribute

to increasing amount of extreme rain events in the two ocean basins, with more pronounced signal in the North Atlantic Ocean than the Northwest Pacific, in part due to the larger increasing in warm pool size in the former. Despite well founded theoretical expectation and modeling projections, a long-term (> decades) trend in observed TC related rainfall has not been established [Knutson et al. 2010].

In this study, possible long-term trends in TC related rainfall is examined for all the ocean basins from 1980 to 2007 using GPCP data set and historical storm track data. Section 2 describes the data and methodology. Section 3 examines the relationship between TC rain and TC intensity from more recent high resolution TRMM data and GPCP pentad data. Section 4 shows results of long-term trend in TC rain. Section 5 examines trends in large-scale environment that may be responsible for the observed changes in TC rainfall. Section 6 summarizes the results.

1. Data and methodology

The precipitation data used in this study include the pentad rainfall from the Global Precipitation Climatology Project (GPCP) for 1979–2007 [Xie et al. 2003], the 3-hourly Tropical Rainfall Measurement Mission (TRMM) Multi-satellite Precipitation Analysis (TMPA) data for 1998–2007 [Huffman et al., 2007]. The 3-hourly TMPA data is used to generate daily gridded precipitation data. The 6-hourly best storm track data for the North Atlantic, Northeast Pacific are from the National Hurricane Center [Jarvinen et al. 1984] and those for the Western North Pacific, Northern Indian Ocean and Southern Ocean are from Joint Typhoon Warning Center [Chu et al., 2000], with a correction of wind speed [Emanuel, 2005]. Data for sea surface temperature (SST) are from the Hadley Center [Rayner et al. 2003]. The NCEP-NCAR Reanalysis-1 [Kalnay et al., 1996] surface air temperature and

120 vertical temperature, humidity, and wind profiles are used to compute changes in TC-related
121 large-scale environmental factors such as vertical wind shear, relative humidity, atmosphere
122 instability and the Maximum Potential Index (MPI). The spatial resolution is 2.5^o latitude x
123 2.5^o longitude for GPCP, NCAR-NCEP Reanalysis, 0.25^o x 0.25^o for TRMM, and 1^o x 1^o for
124 SST.

125 For this study, we estimate the TC-related rainfall for each storm over its life-time
126 (hereafter denoted as TC-rain) using the 6-hourly storm track data. Following Larson *et al*.
127 [2005] and Rodgers et al. [2000, 2001], we define TC-rain as the accumulated amount that
128 falls within an area of 500 km radius, from the center of the TC within the same day (for
129 TRMM data) and the same pentad (for the GPCP pentad data) along the entire track. TC rain
130 estimated from TRMM 3B42 is found to be higher than those estimated from TRMM Radar
131 (2A25) and Microwave imager (2A12) estimates, probably due to overestimate of rainfall by
132 IR-based rainfall retrievals for high and cold clouds [Jiang and Zipser, 2010]. However,
133 because of GPCP's coarse spatial and temporal resolutions, counting the entire pentad as TC-
134 rain can result in some over-estimation of actual TC-rain because non-TC related rain might
135 occur within the same pentad for the grid box. As a result, TC-rain amount calculated from
136 GPCP pentad data is more than those estimated from TRMM TMPA for the same pentad.
137 Since latent heat is released in rainfall, TC-rain can be identified as the total energy generated
138 by a given TC. To facilitate comparison with other forms of energy, hereafter, we convert
139 the TC-rain amount to the unit of Energy Year (EY = 5.10×10^{20} Joule), which is the
140 estimated world primary energy consumption in 2007 (http://eia.gov/aer/txt/ptb1103.html).

141 Figure 1 shows scatter plots of TC-rain estimated from TRMM and GPCP data for
142 different TC categories according to the Simpson-Saffir classification. The GPCP estimates

are systematically higher than that of TRMM by 30-40 percent for all hurricane categories, possibly due to the coarse spatial and temporal resolution of the GPCP data. However, within GPCP there are no systematic differences among TC categories, and for different oceans basins (figure not shown). Therefore it is reasonable to assume that despite its coarse estimate, the GPCP estimate of TC-rain would be self-consistent over time and can be compared over different ocean basins.

Another concern related to the use of GPCP pentad data has to do with temporal inhomogeneity inherent in many long-term satellite data sets [Lau et al., 2008; Zhou and Lau, 2010]. The GPCP rainfall is a merged product that combines available surface rain gauge and operational satellite rainfall estimates to provide a state-of-the-art, multi-decadal global dataset for climate studies [Adler et al., 2003; Xie et al., 2003]. Examination of the pentad data shows significant shifts in tropical rainfall Probability Distribution Function (PDF) with notably more extreme rainfall after inclusion of SSM/I data in 1987 [Zhou and Lau, 2010]. However, the TC-rain data subset we construct for this study does not show any obvious bias between pre-SSM/I and post-SSMI periods (see Figure 3), presumably the bias are embedded more in other heavy rainfall systems such as ITCZ and monsoons, which are not included in our TC-rain construction. While uncertainties undoubtedly exist with respect to some inhomogeneity in the GPCP data, we are reasonably sure that the qualitative results regarding TC-rain are not affected.

2. TC-rain versus TC-intensity

Numerical simulations suggest that TC rainfall will increase as storm intensity increases [Knutson and Tuleya, 2004]. TC rain amount over the life-time of a storm, defined as TC-rain, depends on multiple factors governing storm intensity and duration. The radial

distribution of azimuthally averaged instantaneous rain rates from storm center shows high correlation with storm intensity [Lonfat et al., 2004], but they are strongly modulated by vertical wind shear, total precipitable water, horizontal moisture convergence, ocean surface flux and topography [Lonfat et al., 2007, Jiang et al., 2008]. So far no study has examined the relationship between TC-rain and storm intensity. Figure 2 shows the mean and standard deviation of TC-energy (TC- rain in units of energy) per storm versus the Simpson-Saffir storm category based on GPCP and TRMM TMPA data. TC-energy increases almost linearly with storm intensity, with TS and Category 1, 2 storms on average generating less than 2-5x10^{20} Joule of energy (0.5~1.0 EY) per storm, while for Category 3, 4 and 5, producing 5-7 x10^{20} Joule (1.0~1.5 EY) per storm (Figure. 2a). The more concurrent relationship between daily mean storm wind (averaged from 6 measurements per day) versus daily storm rain also shows positive correlation (Figure not shown), as reported by [Lonfat, 2004 and Jiang et al., 2008]. Large standard deviations are expected due to many other factors affecting TC-rain [Jiang et al., 2008]. The mean TC-rain from GPCP is larger than that from TRMM (Figure. 2b) for the same reasons discussed before. The above results demonstrate that GPCP and TRMM TC-rain data have similar properties with respect to TC intensity for the overlapping period and for all rainfall categories, providing some reassurance that GPCP TC-rain can be used for studies for the longer data period (1979-2007).

3. Recent trends in TC-Rain

In order to examine the trend in TC-rain for each basin and for different TC categories, we compute TC-rain from each category and for each ocean basin. The total TC-rain for each basin is calculated by adding the TC-rain from all the storms in the year from

January to December for the northern hemisphere. For the southern hemisphere, the tropical cyclone year starts from the previous July to current June. Figure 3 shows the global total number of TCs and TC-energy from each storm category from 1980 to 2007. The linear trend of total TC number and TC-energy are computed by linear regression. Globally the total number of tropical storms (TS) increases slightly by 3.8% per decade, with 90% confidence level (c.l.) from the beginning to the end of the data period. The TC numbers in Category 1, 2 and 3 decrease by 6.7%, 13.3% and 17.6% per decade, respectively at 90% c.l.. For Category 4 and 5, the TC numbers increases by 21% and 42% per decade, respectively, with 99% c.l.. These trends are consistent with Webster et al. [2005], but substantially higher than Klotzbach [2006] and Kossin et al. [2007]. The TC energy, converted from TC-rain, generally follows the trend of TC number. However, for TS and Category 4 and 5 storms, the percentage increase of TC energy is 6.2%, 24.8%, and 43.2% per decade, respectively, slightly higher than the corresponding percentage increase in TC number. For Category 1, 2 and 3 storms, the decrease in total TC-energy is less than the rate of decrease in TC number and statistically insignificant, indicating that TC-rain-per-storm might have increased in all the categories. Indeed, calculation shows that the mean energy per storm has increased by 2.6% for TS and by 9.5% for Category 3 TCs (figures omitted).

To examine the trend of TC-rain in each basin, we divide the TCs into 3 groups: TS, Cat 1-3, Cat 4-5, identified as weak, intermediate and intense storms, respectively. This grouping is consistent with the previously discussed linear trends within each group, and has the advantage of enabling relatively homogeneous number of samples in each group. To focus on the long-term (>decadal) changes, we compute the TC-rain and related statistics separately for two equal halves of 14 years each, i.e., 1980-1993, and 1994-2007, and

compare the statistics between the two halves. Figure 4 shows the TC numbers in each group in the first and second half of the period for each basin and global total (All-TC). For the North Atlantic, TC numbers in all categories has significantly increased from the first to the second period. The percentage increase for TS, Cat 1-3, Cat 4-5, and All-TC are 59%, 27%, 149% and 53%, respectively, all significant at 90% level. For the Northwest Pacific, the numbers of TS and Cat 4-5 have increased by 31% and 25%, respectively, while the storm of medium intensity (Cat 1-3) has decreased by 23%. Overall the total TC number still shows a significant increase of 8%. For the Northeast Pacific, TC counts in all groups have decreased, with the number of medium TCs showing a pronounced and significant decrease of 36%, culminating in a total basin-wide reduction of 23%. The inverse relationship between TC activities in Northeast Pacific and North Atlantic is consistent with previous study which reported out-of-phase variations of TC activities in the two ocean basins on both interannual and multi-decadal time scales due to response to opposite changes of atmosphere instability and vertical wind shear associated with ENSO and Atlantic Multi-decadal Oscillations [Wang and Lee, 2009; 2010]. For the Southern Oceans (including both the Southern Indian and the Southern Pacific Ocean), there is a significant increase in the number of Cat 4-5 storms, but not in TS and Cat 1-3 storms. Compared to other ocean basins, the Northern Indian Ocean has the least number of TCs with an average of 4 to 5 per year. Here we note a significant increase of Cat 1-3 storms and Cat 4-5 storms in Northern Indian Ocean. However because of the small number of TCs, the Northern Indian Ocean storms have little effects on the global statistics. Globally, both TS and Cat 4-5 have significant increase in numbers while Cat 1-3 has a 13% decrease. The global total number of TC has a small but significant 5% increase.

The TC-energy by category shows similar patterns as the total number, indicating that total numbers of TC are dominating the TC energy (Figure 5). It is interesting to note that 4 out of 5 basins (Northeast Pacific being the exception), the TC-energy in Cat 4-5 storms has increased. Globally, the increase in TC-energy from Cat 4-5 has significantly increased by 54%, considerably faster than the rate of increase of the TC numbers (Figure 4). The global total TC –rain from all TCs has also increased by a significant 14% (90% c.l.). This suggests that overall there is stronger signal, or higher sensitivity of TC-rain compared to TC number to the changing tropical environment (see further discussion in Section 5). Figure 6 shows the change in energy per-storm (EPS) for each basin and the global total, by storm categories. Over all ocean basins, there is no significant change in EPS for TS. For Cat 1-3, only two ocean basins, *i.e.*, the North Atlantic and the Southern Oceans, show significant 39% and 15 % increase in EPS, respectively. Interestingly, there is a significant reduction in Cat 1-3 EPS over the Northeast Pacific. For Cat 4-5 storm, only the Northwest Pacific shows significant increase. Globally, there is a significant overall 8% EPS increase for Cat 4-5, and 8% increase for all categories. Further computations have shown (figures omitted) that there is no significant increase in TC duration, implying that the EPS increase is largely due to heavier TC-rain, with more latent energy release over the approximately same storm life-span for the two periods.

The systematic change in EPS during the two periods is further illustrated by examining the change in the mean probability distribution functions (PDFs) of rain-per-storm from the first to second period (Fig. 7). Notably Northwest Pacific has the most energetic (wettest) storm, with the top 10% TC-rain EPS threshold exceeding 2.7 EY, followed in order by the Southern Ocean (2.0 EY), the North Atlantic (1.9 EY), the Northeast Pacific (1.5

EY) and the least energetic Indian Ocean (1.4 EY). Globally, 50% of the storm produced more than an equivalent of 1.0 EY of latent energy, while 10% of the storms produced close to 2.2 EY. The difference of PDF shows clearly that there is an internal redistribution of the TC-energy among storms within each basin during the two periods. Over the North Atlantic and Southern Oceans, the PDF-difference suggests a shift of the rainfall spectrum to the right, *i.e.*, more frequent occurrence of energetic storms and less of weak (below 50th percentile) storms. On the other hand, the Northwest Pacific and Northeast Pacific show a flattening of the PDF, *i.e.*, increased frequency of occurrence of the most and the least energetic storms respectively, coupled with a reduction in moderately energetic storms. Interestingly, the PDF difference in the Northern Indian Ocean suggests a shift towards a sharpening of the PDF toward the intermediate and highly energetic storm. Here the small sample size may have contributed to large uncertainties towards the tail end of the spectrum (EY>2). The internal redistribution of the TC-rain PDF may also be affected by inter-basin teleconnection through adjustment in the large scale tropical circulations to long-term climate forcing, affecting the environment for TC development (see further discussion in Section 5). The net result of these redistribution and adjustment processes is a shift in the global EPS PDF, with an increase in more energetic storm (EY >1.5 EY), and a reduction in the lesser and moderately energetic storms (EY<1.5 EY), over all major tropical oceans.

4. Long-term changes in the large-scale environment

It is well known that the global or basin-scale tropical cyclone activities are affected by large-scale environment such as sea surface temperature (SST), vertical wind shear, and atmospheric stability [Gray 1968, 1984; Landsea et al., 1998; Shapiro and Goldenberg, 1996; Cheung, 2004; Vecchi and Soden, 2007; Chan 2009]. For individual TC, the moisture

content in the atmosphere and moisture convergence are important factors affecting storm rainfall [Jiang, 2008; Knutson et al., 2010]. To examine various large-scale environmental factors that might affect the basin total TC rainfall, we compute the linear trends of quantities that are known to affect tropical cyclone formation, genesis and intensity. These include SST, vertical wind shear (magnitude of vector difference of horizontal wind between 850 mb and 200 mb), sea level pressure, mid-troposheric relative humidity, and the Maximum Potential Intensity (MPI) for velocity [Emanuel, 1986; 1995]. The MPI is a measure of the thermodynamic limit on the intensity of a storm based on sea surface temperature and atmospheric temperature and moisture profiles. The trends are computed for the period 1980-2009 for July-November (JASON) and December-April (DJFMA) for the TC seasons in the northern and southern hemispheres respectively.

Figure 8a shows that in JASON, there is a widespread warming trend over the tropical and subtropical Pacific, the Indian Ocean and the North Atlantic, and cooling over the eastern and southeast Pacific, South Atlantic and the southwestern Indian Ocean. The magnitude of the SST increase in the North Atlantic TC domain (dotted rectangle in Figure. 8a), including the Maximum Development Region (MDR, 10^{o}N-20^{o}N, 20^{o}W-85^{o}W) is notably the largest over the other major basins. The lesser warming over the western Atlantic and the Gulf of Mexico region may reflect the increased occurrence of more energetic TCs, whose stronger surface winds could cool the surface ocean by enhanced Ekman upwelling. The Northwest Pacific TC domain generally lies under warmer water in recent decades, but the large increase in SST occurs in the midlatitudes around 35°N-40°N outside of the TC-domain. Similarly a large body of warmer water is found in the South Oceans domain (Figure. 8d) in the region of the South Pacific Convergence Zone. The warmer water

enhances evaporation, and may have contributed to the more energetic storms found in the North Atlantic, the northwestern Pacific and the Southern Oceans. In contrast, a large area of cooling SST is found in the Eastern Pacific TC domain possibly a contributing factor to the decreasing trend in the TC number and TC rainfall in the Northeast Pacific. Over the Indian Ocean TC domain, the SST signal seems to be quite weak.

In JASON, the atmospheric vertical wind shear trend pattern shows near- zonal bands of negative and positive features (Figure 8b). The negative trends appear along the equator while the positive trends appear in the margin of ITCZ, probably associated with the shift of ITCZ and Hadley circulation [Zhou et al., 2011]. Large reduction of vertical wind shear, favorable for enhanced tropical cyclone activities is found in the tropical Atlantic, particularly over the MDR. Most of the TC domain in the northern Indian Ocean observes decreased wind shear, while the TC domain in the northwest Pacific has a band of increasing wind shear near 20^{o}N surrounded by reduced wind shear to the south and the north. On the contrary, the TC domain in the Northeast Pacific is dominated by increasing vertical wind shear, which suppresses tropical cyclone activities. For the DJFMA season, the wind shear trend over the TC domain of the Southern Oceans (Fig. 8e) is generally negative especially in the equatorward side of the domain, favoring TC genesis there. All basins in the northern hemispheres, except the Northeast Pacific, show positive MPI trend, indicating a tendency for increased TC development. In the Northeast Pacific, an area of negative trend in the MPI is found, consistent with suppressed TC activities in this basin as noted in discussions in previous sections.

Table 1 shows a summary of the percentage change of TC rainfall and the 5 major large-scale environmental factors *i.e.,* SST, wind shear, sea level pressure, mid-tropospheric

331 relative humidity, and MPI averaged over different ocean domains (as marked by dotted
332 rectangles in Fig. 8). The percentage changes per decade are computed from the slope of
333 linear regression for the period 1980-2007. The North Atlantic shows the strongest
334 alignment of factors favoring increased TC activities. Three out of the 5 factors show strong
335 (>99% c.l.) in the linear trends, i.e., increased SST, reduced sea level pressure, and increased
336 MPI. All these three factors, together with a significant reduction in vertical wind shear (>90%
337 c.l.) may account for the significant increase (>95.8%) in TC rain in the North Atlantic. For
338 other ocean basins, the trend signals are generally weaker and alignments are not as clear.
339 To provide a quantitative assessment of the degree of alignment of factors among ocean
340 basins, we use an *ad hoc* ranking scheme, by numerically assigning a number from 1 to 5 for
341 each ocean basin and for each factor. In this scheme, #1 representing the largest percentage
342 change per decade favoring TC formation, and #5 the lowest, with the proper sign of the
343 trends taking into account. For example, the North Pacific ranks #1 in both sea surface
344 temperature and sea level pressure, having the largest percentage changes in SST (+1.9 %)
345 and SLP (-0.09%) respectively, and also #1 in wind shear with the strongest reduction in
346 wind shear (-4.2%) among all oceans. The cumulative score for each ocean basin is then the
347 sum of the ranks for all five factors. Accordingly, the range of cumulative score is 5 to 25,
348 with the lower score showing the more alignment of factors favoring enhanced TC activities.
349 Based on the cumulative score (Table 1), the North Atlantic and the Northeast Pacific ranks
350 as the most favorable and least favorable for enhanced TC activities respectively. The two
351 most important factors in the Northeast Pacific that are in sharp contrast to other ocean basins
352 are the large positive wind shear (+4% per decade), and the least value of MPI. These two
353 factors could be key to the significant reduction in TC rainfall (-36.7%) over the Northeast

Pacific. This is consistent with Wang and Lee [2009, 2010], which showed increased TC activities in the North Atlantic coupled to reduced TC activities in the Northeast Pacific, possibly through changes in the Walker Circulation [Zhou e al., 2011]. In the Northwest Pacific, contributing factors favoring increased TC-rain include increased MPI and SST, and reduced SLP and wind shear. However, a reduced mid-tropospheric relative humidity (-0.3%) may oppose TC development there. In the Southern Oceans, a number of factors, *i.e.,* SST, wind shear and MPI, would favor TC activities and TC-rain, but none of these factors ranked the strongest among ocean basins. In the Northern Indian Ocean, moderate increase in SST and MPI, and moderate reduction of wind shear and SLP tend to favor TC activities, but the small reduction of RH may oppose the tendency. Overall, for the Northwest Pacific, Northern Indian Ocean and Southern Oceans, the mixed signals in ambient environmental trends and possible compensations among competing factors (for or against TC development) are consistent with the moderate increase, *i.e*., +21.3%, +53.8%, + 22.2%, respectively found in these ocean basins. In addition, the weak signal in TC-rain in Northwest Pacific has low confidence level due to the previously documented large interannual and inter-decadal variability [Chan 2006, 2009; Lau et al. 2008] (Table 1).

6. Summary and discussion

Using pentad GPCP data, we have estimated rainfall associated with tropical cyclones for all storms from 1980 to 2007 from major ocean basins and examined the long-term trends of tropical cyclone rainfall by storm categories in each basin and in the global mean. From linear regression, we find that globally, tropical cyclone associated rainfall has increased significantly for TS and for Category 4 and 5 by 6.2%, 24.8% and 43.2% per decade, while

decreased by 0.8 %, 9.2% and 5.5% per decade for Category 1, 2 and 3 storms, respectively. The trend in TC rainfall in each category is largely determined by the trend in TC numbers, but the percentage increase in rainfall is larger than the percentage increase in TC numbers. Accumulated total TC rain for all tropical cyclones has a positive trend (8.4% per decade) over the entire tropics.

Large differences in the TC-rain statistics exist among individual basins. The North Atlantic observes increases in both TC number and TC rainfall in weak (TS), intermediate (Cat 1-3), and intense (Cat 4-5) storms, while the Northeast Pacific shows decrease in storm number and storm rain amount for all TC categories. This result is consistent with previous studies [Wang and Lee 2009, 2010] which found an apparent inverse relationship between TC activities between the North Atlantic and Northeast Pacific. The Northwest Pacific observes increases in weak and intense storms while decreases in intermediate storms. Both the Indian Ocean and Southern Oceans show significant increase in the number of intense TC and the associated TC-rain. All basins except the Northeast Pacific show significantly increased TC-rain in Cat 4-5 storms. There is a significant (90% c.l.) increasing trend for energy-per-storm in Cat 1-3 storms in the North Atlantic, and Southern Oceans, and in Cat 4-5 storms in the Northwest Pacific. In contrast, a significant decreasing trend is found in Cat 1-3 storms in the Northeast Pacific. Analyses of TC-energy PDFs finda shift towards greater number of energetic storms at the expense of less energetic TCs is found in the North Atlantic and the Southern Ocean. Over the Northwest and Northeast Pacific, we find a flattening of the PDF, signifying a higher probability energetically for more strong, and weak storms, but less moderate storms. In contrast, Indian Ocean shows a sharpening of the TC rainfall PDF towards moderately energetic storms.

Large-scale environmental variables such as SST, vertical wind shear, sea level pressure, mid-tropospheric humidity, and MPI are analyzed to shed light on the trend differences, and the shift in rainfall PDF among ocean basins. Notably, the North Atlantic observes largest increase in SST and reduction in wind shear, which may explain the largest increase in TC-rain. On the other hand, the Northeast Pacific is unique as the only major ocean basin showing increased vertical wind shear in addition to having the smallest increase in SST, and MPI, which are less favorable for TC activities compared to other ocean basins, consistent with the observed significant negative trend in TC-rain there. For other ocean basins, the trend signals in environment signals are mixed, but overall favoring an increase in TC-rain. Our results suggest that long-term TC-rain changes may be associated with a re-distribution in the latent energy content among the population of storms within and among major ocean basins, associated with the alignment of changes in key large-scale environmental factors [Wu and Wang; 2008]. Further studies are needed to examine the mechanisms of the alignment processes.

The present results are consistent with recent numerical modeling experiments indicating increase in number of simulated high-intensity TCs and increasing TC rainfall in a warming environment [Knutson and Tuleya 2004; Bengtsson et al., 2007; Knutson et al, 2010]. However, large interannual variability in TC activities and short duration of satellite data make it difficult to infer long-term relationship between tropical cyclone rainfall and global warming. Therefore we cannot extrapolate our results to the pre-satellite period, e.g., active TC activity in North Atlantic during late 1920s and late 1960s [Goldenberg et al. 2001; Zhang and Delworth 2009]. For Northwest Pacific, large decadal variation seems to dominate the variation in the last three decades. Therefore, even using the state-of-the-art

multi-decadal rainfall data set, the record length is still too short for a definitive assessment of the long-term trend in TC-rain [Lau et al., 2008]. Furthermore, the results in this work are subject to some uncertainties in the satellite rainfall data as discussed in Section 2. These considerations underscore the need for extending and improving long-term rainfall data sets to obtain reliable estimates of tropical cyclone rainfall such as planned under the Global Precipitation Measurement (GPM) program [Hou et al., 2008].

Acknowledgement This work is supported by the Precipitation Measuring Mission (Headquarter Manager: Dr. R. Kakar), NASA Earth Science Division. NCEP Reanalysis data is obtained from the NOAA/OAR/ESRL PSD, Boulder, Colorado, USA, from their Web site at http://www.esrl.noaa.gov/psd/

References

Adler, R. F. and Coauthors (2003), The version-2 Global Precipitation Climatology Project (GPCP) monthly precipitation analysis (1979–present), *J. Hydrometeor.*, *4*, 1147–1167.

Bengtsson, L. et al. (2007), How may tropical cyclones change in a warmer climate. Tellus, **59A,** 539–561.

Chan, J. C. L. (2006), Comment on "changes in tropical cyclone number, duration, and intensity in a warming environment" Science **311,** 1713.

Chan, J. C. L. (2009), Thermodynamic control on the climate of intense tropical cyclones. Proc. R. Soc. A. **465,** 3011–3021.

Cheung, Kevin K. W. (2004), Large-scale environmental parameters associated with tropical cyclone formations in the western north pacific. *J. Climate*, **17**, 466–484. doi: 10.1175/1520-0442(2004)017<0466:LEPAWT>2.0.CO;2

Chu, J.-H., C. R. Sampson, A. S. Levine, E. Fukada (2002), The Joint Typhoon Warning Center Tropical Cyclone Best-Tracks, 1945-2000. NRL Reference Number: NRL /MR/7540-02-16.
http://metocph.nmci.navy.mil/jtwc/best_tracks/TC_bt_report.html

Emanuel, K. A. (1986), An air-sea interaction theory for tropical cyclones. Part I. J. Atmos. Sci., **42**, 1062-1071.

Emanuel, K. A. (1995), Sensitivity of tropical cyclones to surface exchange coefficients and a revised steady-state model incorporating eye dynamics. J. Atmos. Sci., **52**, 3969-3976.

Emanuel, K. A. (2005), Increasing destructiveness of tropical cyclones over the past 30 years, *Nature*, 436, 686–688.

Goldenberg, S. B., C. Landsea, A. M. Mestas-Nuñez, and W. M. Gray (2001), The recent increase in Atlantic hurricane activity. *Science*, 293, 474–479.

Gray W. M. (1968), Global view of the origin of tropical disturbances and storms. *Mon. Wea. Rev*, ***96***, 669–700.

Gray W. M. (1984), Atlantic seasonal hurricane frequency. Part I: El Niño and 30 mb quasi-biennial oscillation influences. *Mon. Wea. Rev.*, ***112***, 1649–1668.

Groisman, P. Y, et al. (2004), Contemporary changes of the hydrological cycle over the contiguous United Status: trends derived from in situ observations. *J. Hydrometeorology*, 5, 64-85.

Hou, A., C. Kummerow, G. Skofronick-Jackson, and J.M. Shepherd (2008), Global Precipitation Measurement, Chapter 6 in Precipitation: Advances in Measurement, Estimation and Prediction *Springer-Verlag*, 540

Huffman, G.J., R.F. Adler, D.T. Bolvin, G. Gu, E.J. Nelkin, K.P. Bowman, Y. Hong, E.F. Stocker, and D.B. Wolff (2007), The TRMM Multi-satellite Precipitation Analysis (TMPA): Quasi-global, multiyear, combined-sensor precipitation estimates at fine scales. *J. Hydrometeor*., 8, 38–55.

Jarvinen, B. R., C. J. Neumann, and M. A. S. Davis (1984), A tropical cyclone data tape for the North Atlantic Basin, 1886-1983: Contents, limitations, and
uses.NOAA Technical Memorandum NWS NHC 22, Coral Gables, Florida, 21 pp. http://www.nhc.noaa.gov/pdf/NWS-NHC-1988-22.pdf

Jang, H., J. B. Halverson, and E. J. Zipser (2008), Influence of environmental moisture on TRMM-derived tropical cyclone precipitation over land and ocean, *Geophys. Res. Lett.*, *35*, L17806, doi:10.1029/2008GL034658.

Jiang, H., and E. J. Zipser (2010), Contribution of Tropical Cyclones to the Global Precipitation from 8 Seasons of TRMM Data: Regional, Seasonal, and Interannual Variations *J. Climate.*, **23,** 1526-1543.

Kalnay et al. (1996), The NCEP/NCAR 40-year reanalysis project, *Bull. Amer. Meteor*. Soc., 77, 437-470.

Karl, T. R. and R. W. Knight (1998), Secular trends of precipitation amount, frequency, and intensity in the United States. *Bull. Am. Meteorol. Soc.*, 79, 231–241.

Klotzbach P. J. (2006), Trends in global tropical cyclone activity over the past twenty years (1986–2005), *Geophys. Res. Lett*., 33, L10805, doi:10.1029/2006GL025881.

Knutson, T. R., R. E. Tuleya (2004), Impact of CO_2-induced warming on simulated hurricane intensity and precipitation: sensitivity to the choice of climate model and convective parameterization. *J. Climate.* **17,** 3477–3495.

Knutson, T. R.., J. R. , J. l. Mcbride, J. chan, K. Emanuel, G. Holland, C. Landsea, I. Held, J. P. Kossin, A. K. Srivastava and M. Sugi (2010), Tropical cyclones and climate change, *Nature Geoscience*, 3, 157-163.

Kossin, J. P., K. R. Knapp, D. J. Vimont, R. J. Murnane, and B. A. Harper (2007), A globally consistent reanalysis of hurricane variability and trends. *Geophys. Res. Lett.* **34,** L04815.

Landsea, C. W., G. D. Bell, W. M. Gray, S. B. Goldenberg (1998), The extremely active 1995 Atlantic hurricane season: environmental conditions and verification of seasonal forecasts. *Mon. Wea. Rev.,* 126, 1174–1193.

Landsea, C. W., B. A. Harper, K. Hoarau, and J. A. Knaff (2006). Can we detect trends in extreme tropical cyclones? *Science* **313,** 452–454 (2006).

Larson, J., Y. Zhou, and R.W. Higgins (2005), Characteristics of Landfalling Tropical Cyclones in the United States and Mexico: Climatology and Interannual Variability. *J. Climate*, 18, 1247–1262.

Lau, K.-M. & Wu, H. T. (2007), Detecting trends in tropical rainfall characteristics, 1979–2003 *Int. J. Climatol.* **27,** 979–988.

Lau, K.-M., Y. P. Zhou, and H.-T. Wu (2008), Have tropical cyclones been feeding more extreme rainfall? *J. Geophys. Res.,* 113, D23113, doi:10.1029/2008JD009963.

Lonfat, M., F. D. Marks, and S. S. Chen (2004), Precipitation distribution in tropical cyclones using the Tropical Rainfall Measuring Mission (TRMM) microwave imager: A global perspective. *Mon. Wea. Rev.,* 132, 1645–1660.

Lonfat, M., R. Rogers, T. Marchok, and F.D. Marks Jr. (2007), A parametric model for predicting hurricane rainfall. *Mon. Wea. Rev.,* 135, 3086–3097.

Pielke, R. A., Jr., C. Landsea, M. Mayfield, J. Laver, and R. Pasch (2005), Hurricanes and global warming. *Bull. Am. Meteorol. Soc.,* 86, 1571–1575.

Rayner, N. A., D. E. Parker, E. B. Horton, C. K. Folland, L. V. Alexander, D. P. Rowell, E. C. Kent, and A. Kaplan (2003), Global analyses of SST, sea ice and night marine air temperature since the late nineteenth century. *J. Geophys. Res.,* **108,** 4407, doi:10.1029/2002JD002670.

Rodgers, E.B., R.F. Adler, and H.F. Pierce (2000), Contribution of Tropical Cyclones to the North Pacific Climatological Rainfall as Observed from Satellites. *J. Appl. Meteor.,* 39, 1658–1678.

Rodgers, E.B., R.F. Adler, and H.F. Pierce (2001), Contribution of Tropical Cyclones to the North Atlantic Climatological Rainfall as Observed from Satellites. *J. Appl. Meteor.,* 40, 1785–1800.

Shapiro, L. J. and S. B. Goldenberg (1998), Atlantic sea surface temperatures and tropical cyclone formation. *J. Climate.,* 11, 578–590.

Shepherd, J.M., and T. Knutson (2006), The current debate on the linkage between global warming and hurricanes, Geography Compass, Geography Compass, Geography Compass 1 (1), 1–24. doi:10.1111/j.1749-8198.2006.00002.x.

Shepherd, J. M., A. Grundstein, and T. L. Mote (2007), Quantifying the contribution of tropical cyclones to extreme rainfall along the coastal southeastern United States. *Geophys. Res. Lett*., 34, L23810, doi:10.1029/2007GL031694.

Vecchi, G. A. and B. J. Soden (2007), Effect of remote sea surface temperature change on tropical cyclone potential intensity. *Nature*, 450, 1066–1070.

Wang, C., and S.-K. Lee (2009), Co-variability of tropical cyclones in the North Atlantic and the eastern North Pacific, *Geophys. Res. Lett.*, 36, L24702, doi:10.1029/2009GL041469.

Wang, C., and S.-K. Lee (2010), Is hurricane activity in one basin tied to another? EOS, 91, No.10, 9 March 2010.

Webster, P. J., G. J. Holland, J. A. Curry, and H.-R. Chang (2005), Changes in tropical cyclone number, duration, and intensity in a warming environment. *Science*, 309, 1844–1846.

Wu, L., B. Wang (2008), What Has Changed the Proportion of Intense Hurricanes in the Last 30 Years?. *J. Climate*, **21**, 1432–1439. doi: 10.1175/2007JCLI1715.1

Wu, Y. S., and P. Zhai (2007), The impact of tropical cyclones on Hainan Island's extreme and total precipitation. *Int. J. Climatol*., 27, 1059–1064.

Xie P., J. E. Janowiak, P. A. Arkin, R. F. Adler, A. Gruber, R. Ferraro, G. J. Huffman, and S. Curtis (2003), GPCP pentad precipitation analyses: An experimental dataset based on gauge observations and satellite estimates. *J. Climate., 16,* 2197–2214.

Zhang, R., and T. L. Delworth, (2009), A new method for attributing climate variations over the Atlantic Hurricane Basin's main development region. *Geophys. Res. Lett.* **36,** L06701.

Zhou, Y. P., K.-M. Xu, Y. C. Sud, and A. K. Betts (2011), Recent trends of the tropical hydrological cycle inferred from Global Precipitation Climatology Project and International Satellite Cloud Climatology Project data, *J. Geophys. Res., 116,* D09101, doi:10.1029/2010JD015197.

Zhou, Y. P., K. –M. Lau (2010), Tropical rainfall trends from GPCP analyses, *Proceedings of the Forecasting and COAA 5th International Ocean-Atmosphere Conference*, Taipei, June 28-20, 2010.

Table 1. Summary of the percentage change of TC-rain and 5 major large-scale environmental factors averaged over different ocean domains (as marked by dotted rectangles in Fig. 8). The percentage changes are computed from the slope (% per decade) of linear regression multiplied by the number of decades (=2.8) for the period 1980-2007. The TC-rains are computed as total for the TC seasons for JASON, and ONDJF for the northern and southern hemisphere respectively. Trends with confidence levels greater than 90%, 95% and 99% are indicated with superscripts $^{+}$, * and bold fonts, respectively.

Change%	North Atlantic	Northeast Pacific	Northwest Pacific	N. Indian Ocean	Southern Oceans
SST	**1.9**	0.8^{+}	**1.4**	1.0^{*}	**1.0**
WS	-4.2+	4.0^{+}	-3.4	-4.0^{*}	-2.1
SLP	**-0.09**	-0.01	-0.03+	-0.04^{+}	-0.01
RH	2.2	8.3^{*}	-0.3	-0.04	2.5^{+}
MPI	**11.3**	4.6^{*}	**12.1**	**11.0**	**9.6**
Score	8	20	14	15	17
TC-rain	**95.8**	-36.7^{+}	21.3	53.8^{+}	22.2^{+}

Figure captions

Figure 1. TC-rain in energy unit from TRMM versus from GPCP for different TC categories during the overlapping period 1998-2007.

Figure 2. Mean (green bar) and standard deviation (black line) of TC-rain per storm in energy unit for different TC categories from (a) TRMM and (b) GPCP.

Figure 3. Time series of global total TC-rain in energy units (solid line) and TC number (dotted line) for different TC categories.

Figure 4. Annual mean number of TCs from three TC groups and all TCs for the first 14 years (1980-1993, left bars) and latter 14 years (1994-2007, right bars) in each ocean basin and global total. Orange and blue bars indicate significant (above 90% confidence level) positive and negative changes. Numerical values are shown for significant percentage changes.

Figure 5. Same as Figure 4, but for basin total TC-rain in energy unit (EY) from different TC categories.

Figure 6. Same as Figure 4, but for the mean TC-energy per storm for different TC categories.

Figure 7. Frequency distributions of TC as a function of accumulated TC-rain in energy unit (EY) over its life time. The blue lines show the climatological mean distributions over the entire period (1980-2007). The color filled lines show the difference between the latter 14 years (1994-2007) and earlier 14 years (1980-1993), positive in red and negative in green. .

Figure 8. **Left:** Linear trends of (a) SST, (b) vertical wind shear, and (c) MPI for wind in July-November that affect TC activities in the northern oceans from 1980 to 2007.

652 **Right:** the same as the left panels except for trends in December-April that affects
653 TC activities in the southern oceans. The dotted rectangles indicate domains where
654 the mean values of each environmental variables in Table 1 are computed.
655

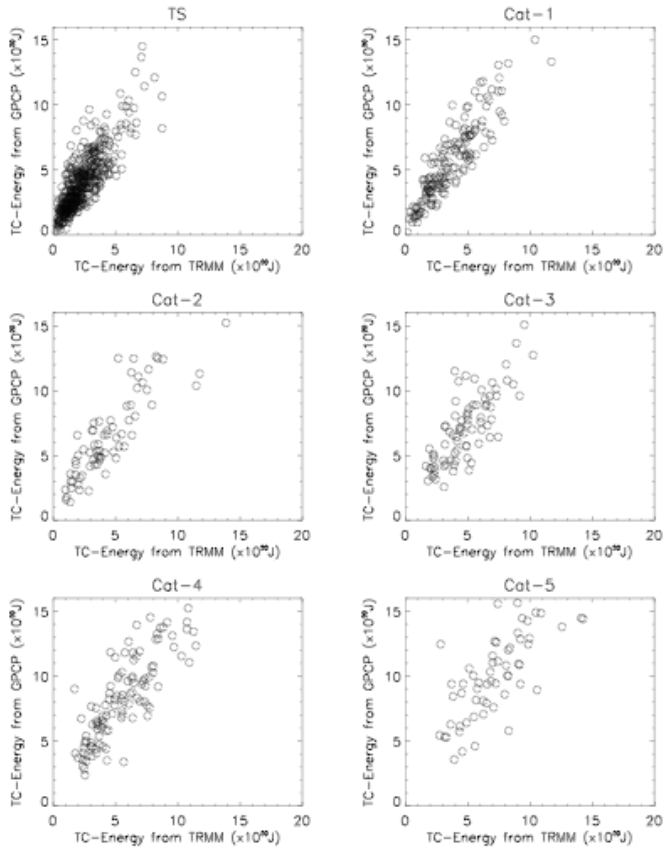

≈

Figure 1. TC-rain in energy unit (10^{+20} Joules) from TRMM versus from GPCP for different TC categories during the overlapping period 1998-2007.

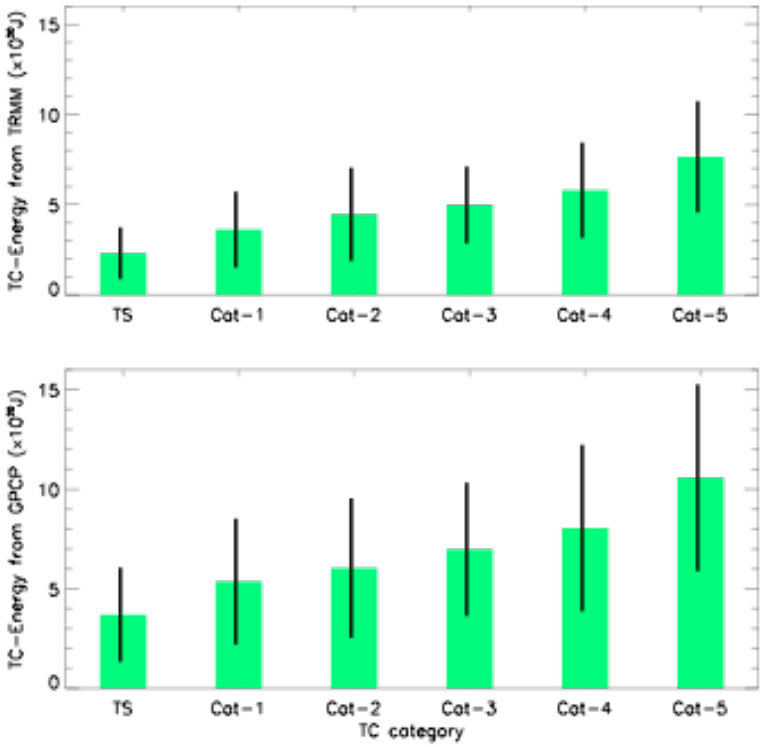

Figure 2. Mean (green bar) and standard deviation (black line) of TC-rain per storm in energy unit (10^{+20} Joules) for different TC categories from (a) TRMM and (b) GPCP.

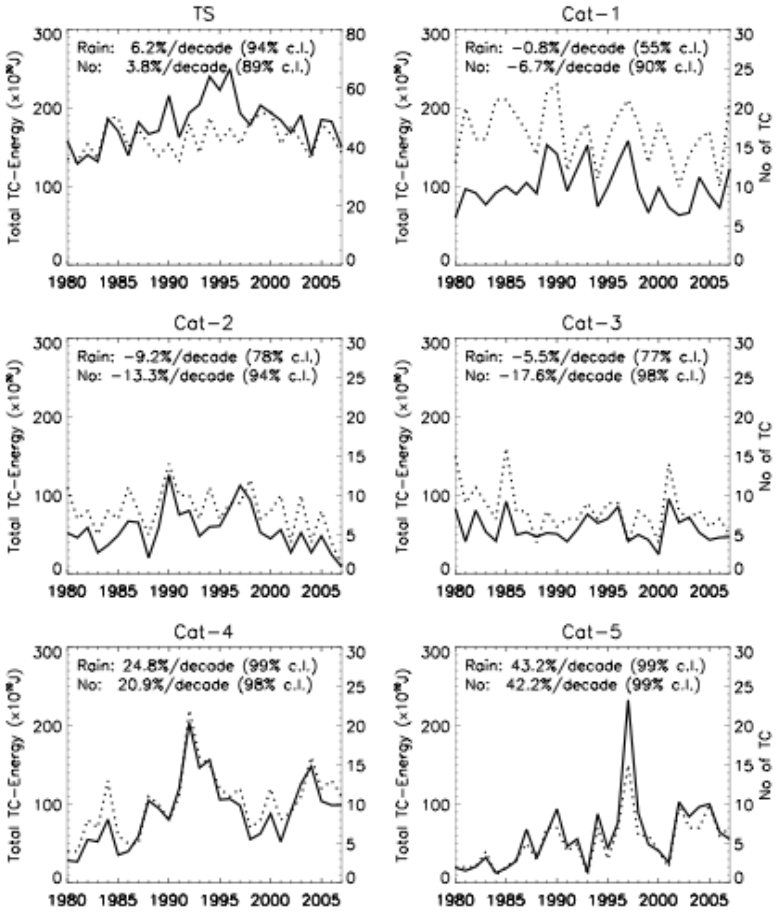

687
688 Figure 3. Time series of global total TC-rain in energy unit (solid line) and TC number
689 (dotted line) for different TC categories.
690
691
692
693

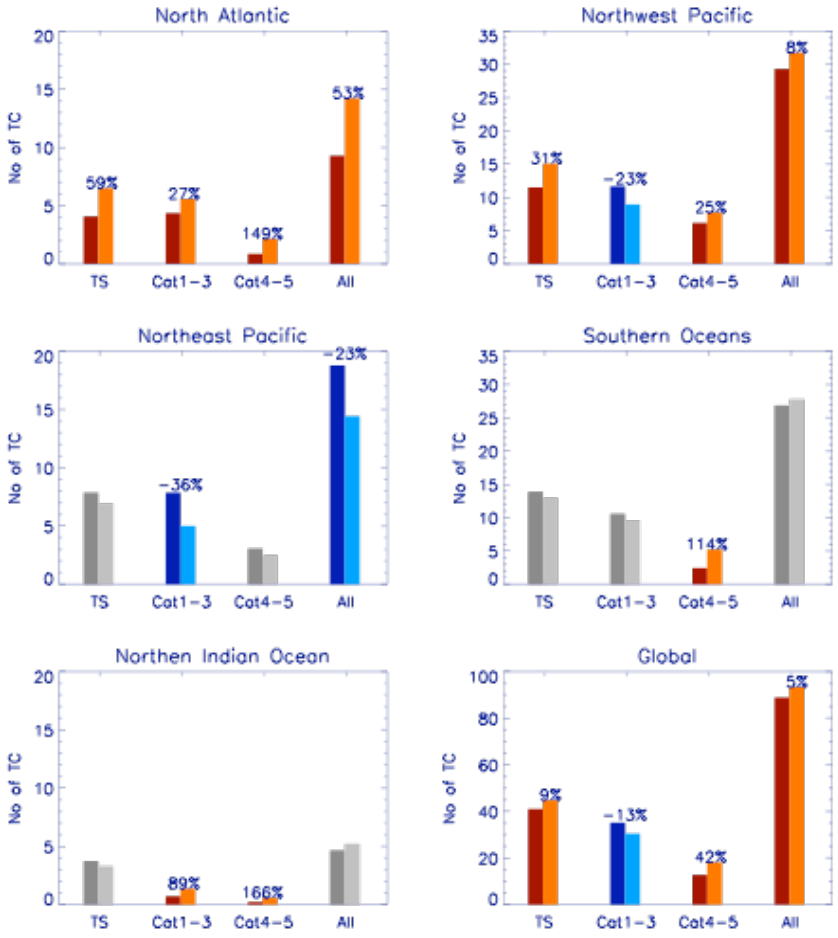

Figure 4. Annual mean TC numbers from three TC groups and all TCs for the first 14 years (1980-1993, left bars) and latter 14 years (1994-2007, right bars) in each ocean basin and global total. Orange and blue bars indicate significant (above 90% confidence level) positive and negative changes. Numerical values are shown for significant percentage changes.

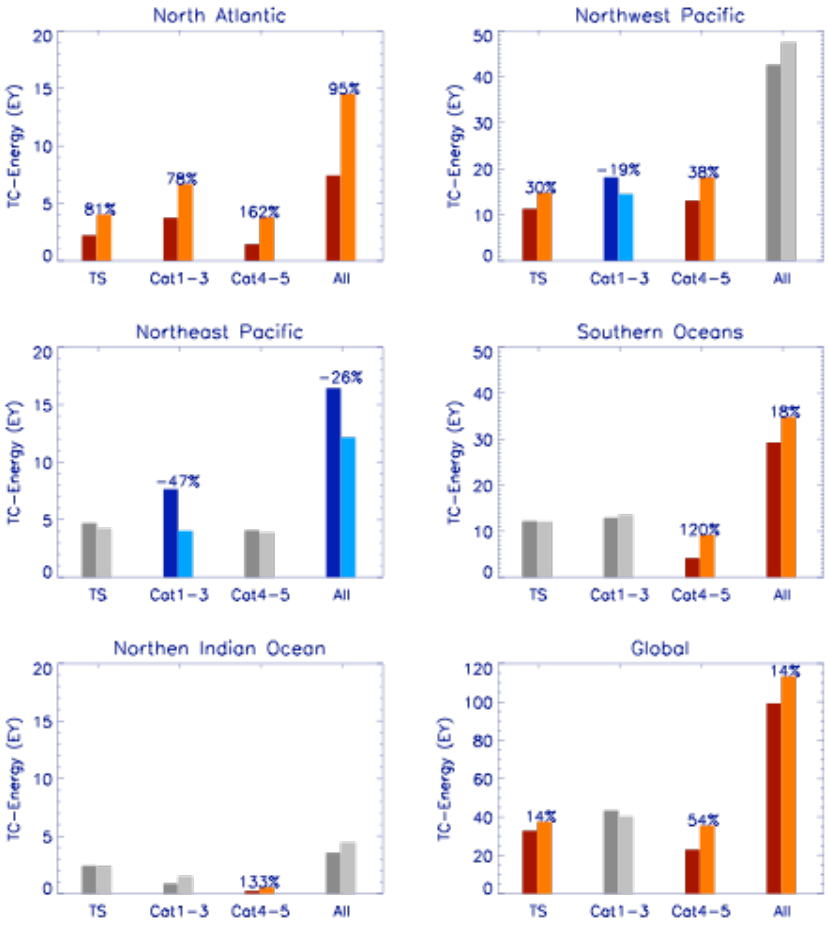

705
706
707 Figure 5. Same as Figure 4, but for basin total TC-rain in energy unit (EY) from different
708 TC categories.
709

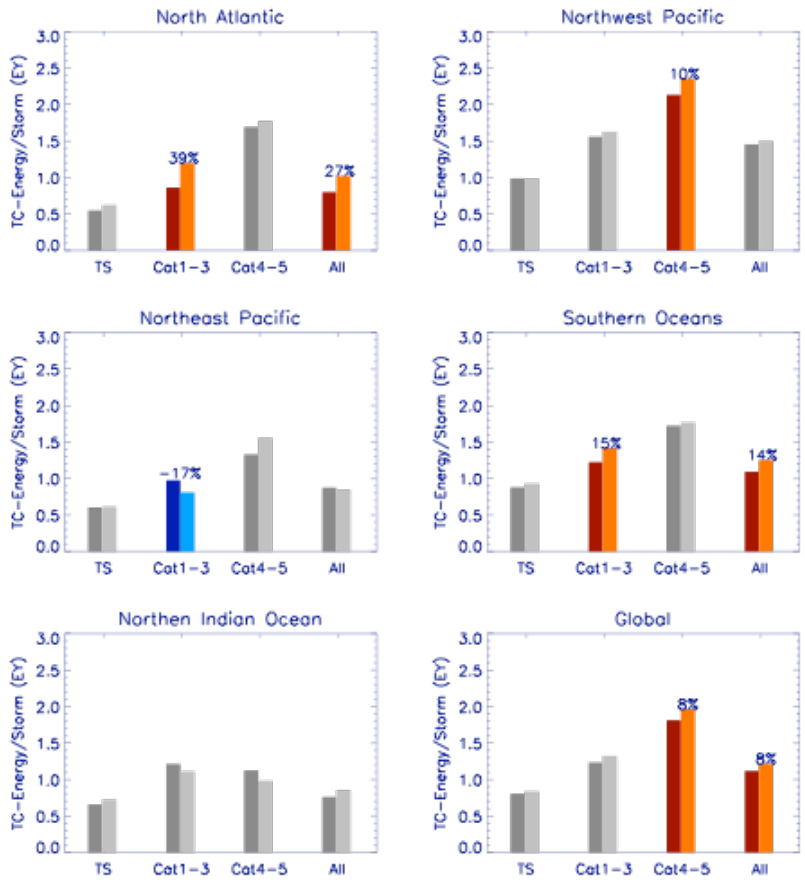

Figure 6. Same as Figure 4, but for the mean TC-energy per storm for different TC categories.

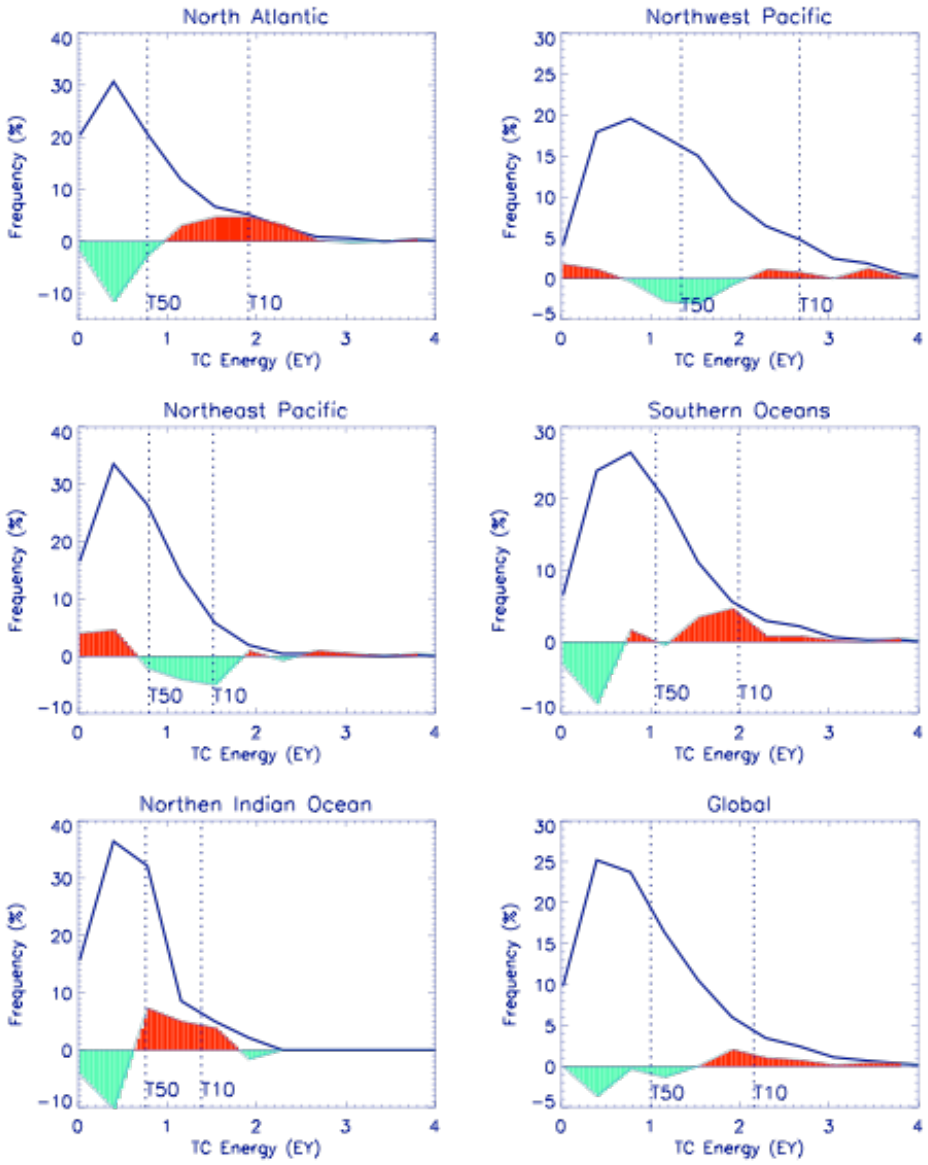

Figure 7. Frequency distributions of TC as a function of accumulated TC-rain in energy unit (EY) over its life time. The blue lines show the climatological mean distributions over the entire period (1980-2007). The color filled lines show the difference between the latter 14 years (1994-2007) and earlier 14 years (1980-1993), positive in red and negative in green. .

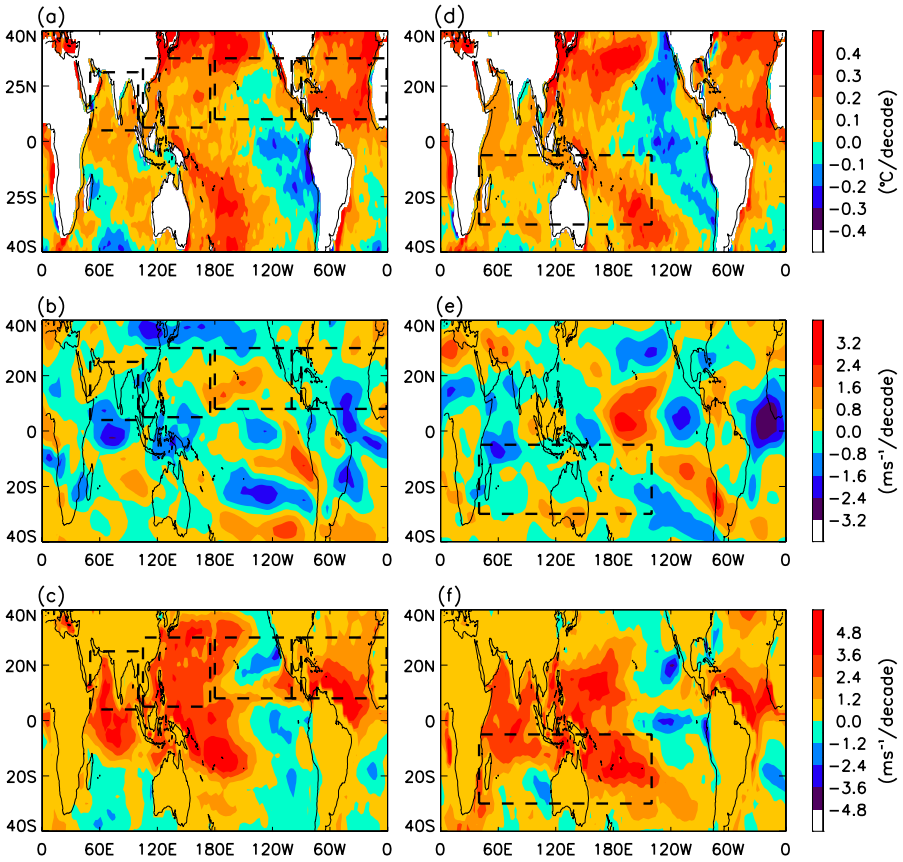

Figure 8. **Left:** Linear trends of (a) SST, (b) vertical wind shear, and (c) MPI for wind in July-November that affect TC activities in the northern oceans from 1980 to 2007. **Right:** the same as the left panels except for trends in December-April that affects TC activities in the southern oceans. The dotted rectangles indicate domains where the mean values of each environmental variables in Table 1 are computed.